4402 *J. Phys. Chem. A* **1997,** *101,* 4402−4408

Theoretical Study of the Reaction of Silyl Radical with Ethylene and Propylene

Andrea Bottoni

Dipartimento di Chimica "G. Ciamician", Universita' di Bologna, via Selmi 2, 40126 Bologna, Italy

Received: October 1, 1996; In Final Form: February 5, 1997⊗

The potential energy surfaces for the reactions of silyl radical $^{\bullet}$SiH$_3$ with ethylene and propylene are studied using both the spin-projected MP2 method (PMP2) with the 6-31G* basis set and the QCISD(T) method with the more accurate 6-311G** basis. For both reactions it is found that the channels leading to the olefin double-bond addition are highly favored with respect to the reaction pathways associated with hydrogen abstraction. These results agree with recent experiments and rule out the hypothesis that hydrogen abstraction and not double addition can be the primary process in the case of propylene. However, in the comparison between ethylene and propylene, it is found that the activation energy for the addition is slightly lower in the latter case than in the former suggesting that in gas phase alkyl substitution activates olefins toward addition by $^{\bullet}$SiH$_3$. The good agreement between the PMP2 and the QCISD(T) results and the experimental results (activation energies and reaction enthalpies) indicates that a PMP2 approach with a basis set of double-ζ quality plus polarization functions (6-31G*) can provide a reliable description for this class of reactions. A simple diabatic model is used to rationalise these computational results. This model indicates the $\pi \rightarrow \pi^*$ triplet excitation energy as the key factor which determines the trend of the gas-phase activation barrier on passing from ethylene to propylene.

Introduction

The addition of silyl radicals to olefin double bonds represents the key step (eq 1)

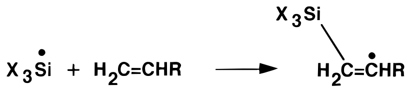

$$\mathrm{X_3\dot{S}i + H_2C{=}CHR \longrightarrow \overset{X_3Si}{H_2C}{=}\dot{C}HR} \qquad (1)$$

in free radical hydrosilylation reaction, which has been for many years, since its discovery, one of the most important methods for preparing organosilicon compounds. A vast amount of experimental work has been carried out on this reaction.[1−4] The experimental data point out that the addition of silyl radicals to alkenes is an easy process according with the strongly exothermic character of the reaction. An experimental determination of the exothermicity provides a value of -16 kcal mol^{-1} for the gas phase addition of Cl$_3$Si$^{\bullet}$ to ethylene.[2] Higher values have been determined more recently for the addition of Me$_3$Si$^{\bullet}$ to several olefins: -26, -27, and -37 kcal mol^{-1} for CH$_2$=CH$_2$, CH$_2$=CHMe and CH$_2$=CHPh, respectively.[1e] Because of this strong exothermicity the addition of silyl radicals to double bonds is an irreversible process at room temperature. The absolute rate constants for the addition of silyl radicals to various olefins have been reported.[3] These data point out that the reactivity is more pronounced for olefins having the double bond next to a π-electron system or to an electron-withdrawing substituent. It has also been found that other reactions such as halogen abstraction can compete with the addition to the olefin double bond. With H$_2$C=CCl$_2$, for example, triethylsilyl radicals react exclusively by addition, while with ClCH=CCl$_2$ the addition is in competition with Cl atom abstraction, and with Cl$_2$C=CCl$_2$ only the Cl transfer is observed.[4]

Recently Loh et al.[1f] studied the gas-phase addition reaction of $^{\bullet}$SiH$_3$ with ethylene, propylene, and propyne. In these experiments silyl radicals were generated by photolysis of BrSiH$_3$ at 193 nm. Initially they found that the rate constant for reaction with propylene was at least 2 orders of magnitude larger than for reaction with ethylene. Since alkyl substitution does not appear to enhance the reactivity of olefins toward addition of trialkylsilyl radicals in solution,[3a] the authors initially suggested that a new reaction channel corresponding to hydrogen abstraction was available in the case of propylene and that the reaction could proceed primarily via hydrogen abstraction rather than addition. However subsequent and more extensive experiments led the authors to conclude that the anomalous reactivity of silyl with propylene was due to the fast reaction of $^{\bullet}$SiH$_3$ with small quantities of radicals generated in the 193 nm photolysis of propylene and that to explain the results no additional reaction channel such as hydrogen abstraction was required.

The present paper has two aims. The first is to assess, using a theoretical approach, the relative importance of the abstraction and insertion processes in the reaction of $^{\bullet}$SiH$_3$ with ethylene and propylene. The second is to determine the effect of methyl substitutions on the activation of the olefinic bond in the addition reaction. To this purpose we investigate in detail the potential energy surfaces associated with the reaction of silyl radical $^{\bullet}$SiH$_3$ with ethylene and propylene using both a spin-projected MP2 and a quadratic Cl approach (QCISD(T)) to take into account the dynamic correlation energy contributions which are essential to obtain reliable energetics.

Computational Procedure

Ab-initio unrestricted Moller−Plesset calculations up to second-order (MP2) were performed with the Gaussian 92[5] series of programs using the 6-31G* basis set[6a] (MP2/6-31G* computational level). In all cases the geometries of the various critical points were fully optimized with the gradient method available in Gaussian 92. The nature of each critical point was characterized by computing the harmonic vibrational frequencies at the MP2 level. As suggested by Sosa and Schlegel,[7] we used spin-projected MP2 energies (PMP2) to cancel the spin contamination which affects mailny the transition structures and which can cause an overestimation of the energy barriers. To obtain a better estimate of the reaction energetics and to assess

---

⊗ Abstract published in *Advance ACS Abstracts,* April 15, 1997.

S1089-5639(96)03013-7 CCC: $14.00 © 1997 American Chemical Society

the reliability of the PMP2 approach, we used the quadratic CI method available in Gaussian 92, including single, double, and triple excitations (QCISD(T)), to carry out single-point computations with the 6-311G** basis set[6b] on the geometries optimized at the MP2/6-31G* level.

Results and Discussion

A. Structures and Energetics. All the results are collected in Tables 1−7 and Figures 1−4. In Tables 1 and 3 we give the absolute and relative energies computed with the 6-31G* basis set at the PMP2 level of theory for the reaction of $^{\bullet}SiH_3$ with ethylene and propylene, respectively. In addition to the energy values we report also the zero-point vibrational energy corrections (ZPE, unscaled), the thermal corrections to enthalpy (H_{th}) at the temperature $T = 298$ K, and the corresponding activation energies and reaction enthalpies (E_a or ΔH). These values can be compared to a good approximation to the experimental Arrhenius activation energies (E_a) and to the experimental reaction enthalpies (ΔH). The enthalpy thermal corrections are given by the following expression

$$H_{th} = \mathrm{ZPE} + E_{vib} + E_{rot} + E_{tr} + RT$$

where E_{vib}, E_{rot}, and E_{tr} are the vibrational, rotational, and translational contributions to the energy, respectively, T is the absolute temperature, and R is the gas constant. The molecular enthalpy is computed as $H = E + H_{th}$, where E is the quantomechanical energy, while the activation energy is obtained from the expression $E_a = \Delta H\# + nRT$, where $\Delta H\#$ is the activation enthalpy and n represents the molecularity of the reaction (2 in the present case). In Tables 2 and 4 we report the energy values obtained for the two reactions at the QCISD(T) level of theory with the 6-311G** basis set. In this case to calculate the activation energy and the reaction enthalpies we use the H_{th} contributions obtained in the frequency computations at the MP2/6-31G* level. We also report in Table 5 the expectation values of S^2 ($\langle S^2\rangle$) obtained at the MP2 level. A complete tabulation of the vibrational frequencies computed for the various critical points is given in Tables 6 and 7. In Figures 1−4 we represent the structures corresponding to the various critical points found on the potential energy surfaces together with the optimum values of the most important geometrical parameters obtained at the MP2/6-31G* level.

We begin our discussion with the results obtained for ethylene. In this case we have located two transition states, TS_1 and TS_2, both characterised by a C_s symmetry. TS_1 corresponds to the addition of the silyl radical to the C−C double bond (Figure 1a), while TS_2 leads to the vinyl hydrogen abstraction (Figure 1b). While in the former case the transition vector corresponding to the imaginary frequency is dominated by the approaching distance r (see Scheme 1), in the latter this vector corresponds to a linear combination of the forming Si−H and breaking C−H bonds. In TS_1 the new forming Si−C bond and the breaking C−C double bond are respectively 2.577 and 1.344 Å while the angle of attack of the radical to ethylene is 97.6°. As a consequence of the formation of the new Si−C bond a considerable rehybridization of the olefin carbon atom C_1 takes place. A measure of the pyramidalization of C_1 is given by the angle ϵ which is 168.1° (ϵ is represented in Scheme 1 and corresponds to the angle between the C−C bond and the $H_1C_1H_1'$ plane; its value is 180° in the planar ethylene). The two methyl hydrogens bonded to C_2 are only slightly bent out of the ethylene molecular plane but in the opposite direction with respect to C_1: the pyramidalization of C_2 is described by the ϕ angle (also defined in Scheme 1), which is 175.8°.

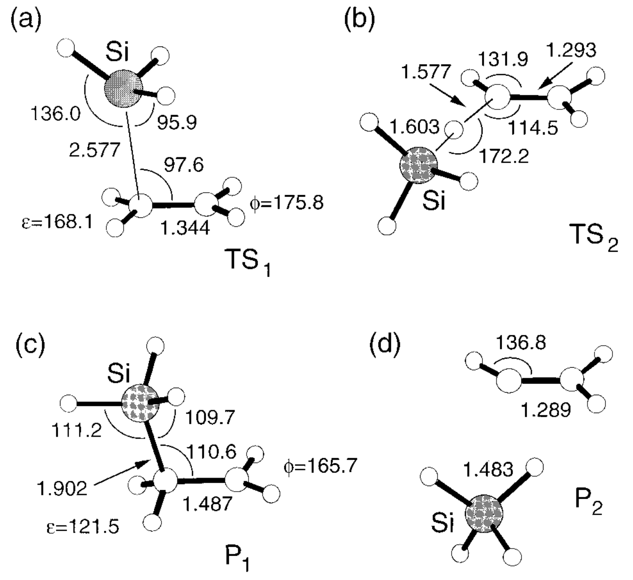

Figure 1. Schematic structures of transition states and products for the reaction $^{\bullet}SiH_3 + H_2C{=}CH_2$. Bond lengths are in angstroms and angles in degrees.

SCHEME 1

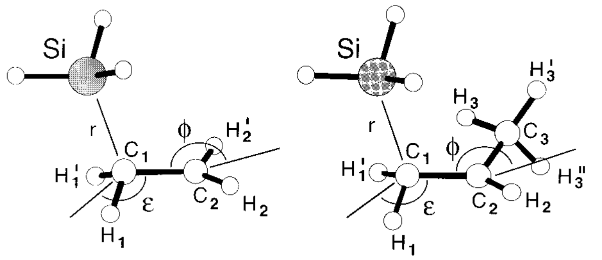

TS_2 is characterized by an almost collinear arrangement of the three atoms involved in the hydrogen transfer, the ∠SiHC angle being 172.2°. The new Si−H bond is 1.603 Å, while the breaking C−H bond is 1.577 Å. The loss of an hydrogen atom causes a significant increase of the HCC angle (131.9°) for the adjacent hydrogen and a decrease of the C−C bond, which becomes 1.293 Å.

The addition product P_1 is a carbon-centered radical (Figure 1c) where the H_3Si group is staggered with respect to the C−C bond. The most significant changes in structural parameters on passing from TS_1 to P_1 is found in a shortening of the new Si−C bond which becomes complete (1.902 Å) and a further lengthening of the C−C bond which loses definitely the double-bond character (1.487 Å). A significant variation is also observed in the ∠HSiC angles which become very close to the characteristic value of the tetrahedral angle (111.2° and 109.7°). The hybridization of the carbon C_1 is now sp^3 ($\epsilon = 121.5°$), and a nonnegligible pyramidalization characterizes also the radical center, the ϕ angle being 165.7°. In Figure 1d we have also reported the structures of the vinyl radical and the silane molecule which represent the abstraction product (P_2). The vinyl radical is characterized, with respect to TS_2, by a further decrease of the C−C bond and a further increase of the ∠HCC angle, which become 1.289 Å and 136.8° respectively.

For the reaction between $^{\bullet}SiH_3$ and propylene, we have located seven different transition states. Two of them, TS_1 and TS_2, lead to the addition of the silyl radical to the olefin double bond at the C_1 and C_2 carbon atoms respectively, and in both cases the transition vector corresponding to the imaginary frequency is dominated by the approaching distance r. Even if TS_1 (Figure 2a) has lost the C_s symmetry, it is very similar to

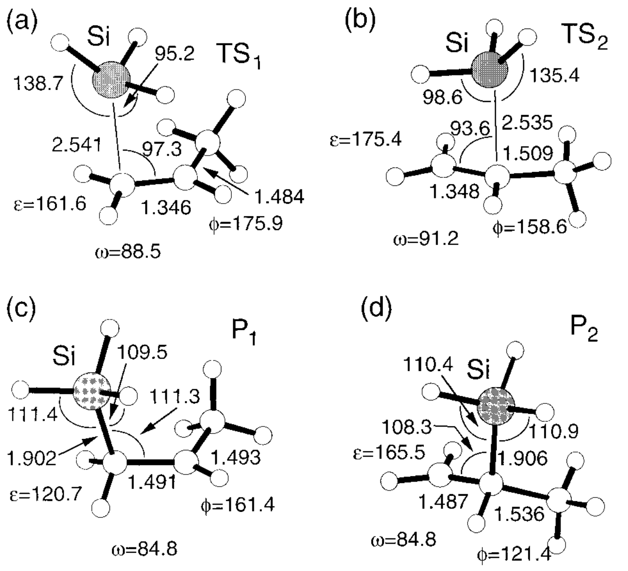

Figure 2. Schematic structures of transition states and products for the addition reaction $^{\bullet}SiH_3 + H_2C{=}CHCH_3$. The dihedral angles ω are defined as follows: (a) $\omega = \omega[Si(C_1C_2)C_3]$; (b) $\omega = \omega\,[Si(C_2C_1)H_1']$; (c) $\omega = \omega[Si(C_1C_2)C_3]$; (d) $\omega = \omega[Si(C_2C_1)H_1']$. Bond lengths are in angstroms and angles in degrees.

the analogous transition state located in the case of ethylene. The direction of attack of the radical lies in a plane that is approximately orthogonal to the propylene molecular plane as indicated by the dihedral angle ω between the two planes SiC_1C_2 and $C_1C_2C_3$ which is 88.5° (this dihedral angle is identified by the symbol $\omega[Si(C_1C_2)C_3]$). In this structure the angle of attack of the silyl radical is 97.3°, the new forming Si−C bond is 2.541 Å, and the C−C bond is 1.346 Å. Also in this case a significant rehybridization of the C_1 carbon atom takes place (the ϵ angle is 161.6°) and the incipient radical center is slightly pyramidal (the ϕ angle is 175.9°). TS_2 (Figure 2b) is characterized by similar values of the two bonds involved in the reaction: Si−C is 2.535 Å, and the olefin bond is 1.348 Å. The steric repulsion between the silyl group and the adjacent methyl group is probably responsible for a smaller value of the angle of attack, which becomes 93.6°. For this structure the dihedral angle ω between the two planes SiC_2C_1 and $C_2C_1H_1'$ ($\omega[Si(C_2C_1)H_1']$) is 91.2° and shows that the direction of attack is approximately orthogonal to the molecular plane.

TS_1 and TS_2 lead to the radical products P_1 and P_2 respectively (Figure 2c,d). The values of the Si−C and olefin bonds are similar in the two molecules, while the $\angle SiC_1C_2$ angle is smaller in P_2 than in P_1 as found in the comparison between TS_2 and TS_1. A more significant difference in the comparison between the two radicals is found in the C_2C_3 bond distance which is 1.493 in P_1 and becomes 1.536 in P_2. The smaller value in P_1 has probably the effect of maximizing the attractive interaction between the singly occupied orbital centered on C_2 and the empty σ_{C-H^*} orbital associated with the C−H bond orthogonal to the molecular plane (C_3−H_3').

The remaining five transition states correspond to the abstraction of the vinyl (TS_3, TS_4, TS_5) and methyl (TS_6, TS_7) hydrogens. In all cases the three atoms involved in the reaction are almost collinear, the $\angle SiHC$ angle being in the range 179.7−171.1°. The transition states leading to vinyl hydrogen abstraction (Figure 3a−c) are planar structures with very similar values of the breaking and forming bonds. As already pointed out for ethylene, the bond angles of the hydrogen atom or the carbon atom that is adjacent to the transferred hydrogen ($\angle H_1C_1C_2$, $\angle H_1'C_1C_2$, and $\angle C_3C_2C_1$ angles) become larger than 130°, and the C−C bond length decreases with respect to the value in free propylene (1.338 Å). It is interesting to point out that, while in TS_3 and TS_5 the C_2−C_3 bond length is about 1.50 Å, in TS_4 this bond becomes shorter (1.480 Å). The shortening of this bond probably maximizes the attractive interaction between the incipient singly occupied sp^2 hybrid orbital and the in-plane empty σ_{C-H^*} orbital of the methyl group.

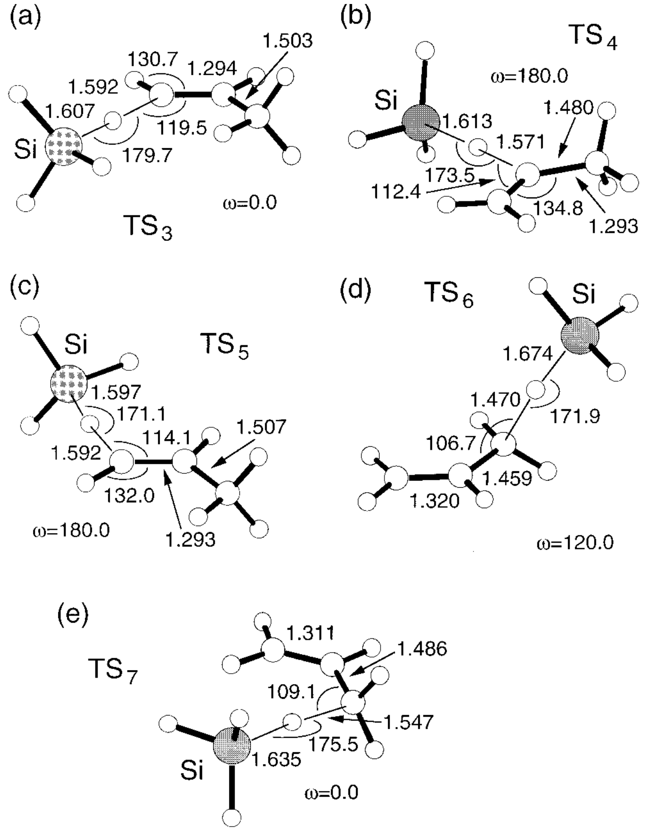

Figure 3. Schematic structures of transition states for the hydrogen abstraction $^{\bullet}SiH_3 + H_2C{=}CHCH_3$. The dihedral angles ω are defined as follows: (a) $\omega = \omega[Si(C_1C_2)C_3]$; (b) $\omega = \omega\,[Si(C_2C_1)C_3]$; (c) $\omega = \omega\,[Si(C_1C_2)C_3]$; (d) $\omega = \omega[Si(C_3C_2)C_1]$; (e) $\omega = \omega[Si(C_3C_2)C_1]$. Bond lengths are in angstroms and angles in degrees.

TS_6 (Figure 3d) and TS_7 (Figure 3e), when compared to TS_3, TS_4, and TS_5, are characterized by a longer Si−H distance (1.674 and 1.635 Å respectively) and a shorter C−H distance (1.470 and 1.547 Å). Thus they show a more reactant-like character than the transition states for vinyl hydrogen abstraction. Another significant feature that deserves to be pointed out is the short C_2−C_3 distance found in TS_6 and TS_7 (1.459 and 1.486 Å respectively). This can be explained by the allylic character of the two transition structures. Furthermore since the two hydrogens not involved in the transfer process are approximately orthogonal to the molecular plane in TS_7 but not in TS_6, this allylic character must be stronger in the latter case than in former, in agreement with the shorter C2−C3 bond length found in TS_6.

The products corresponding to the transition states previously discussed are shown in Figure 4 (for sake of simplicity we have omitted the silane molecule). While TS_6 and TS_7 both lead to the formation of an allyl radical (P6), TS_3, TS_4, and TS_5 lead to three different vinyl radicals (P_3, P_4, and P_5), which are all planar structures with a C_s symmetry. As already pointed out in the case of ethylene, the bond angle adjacent to the radical center is larger than in the corresponding transition state. It is interesting to note that, as found in the comparison between TS_3, TS_4, and TS_5, the attractive orbital interaction between the in-plane sp^2 singly occupied orbital and the $\sigma_{C-H}{}^*$ orbital is

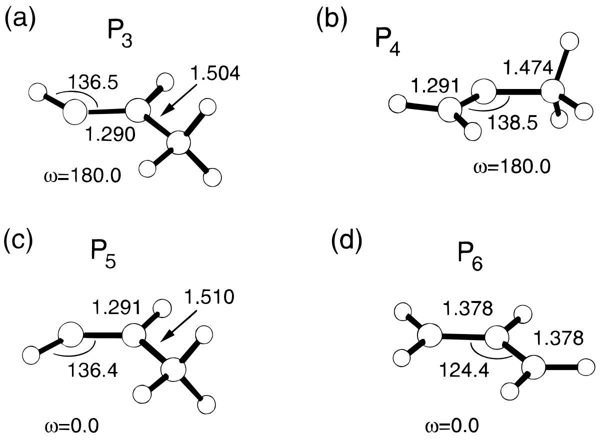

Figure 4. Schematic structures of products for the hydrogen abstraction $^{\bullet}SiH_3 + H_2C{=}CHCH_3$. The dihedral angles ω are defined as follows: (a) $\omega = \omega[C_3(C_2C_1)H_1]$; (b) $\omega = \omega\ [C_3(C_2C_1)H_1]$; (c) $\omega = \omega\ [C_3(C_2C_1)H_1']$; (d) $\omega = \omega[C_3(C_2C_1)H_1']$. Bond lengths are in angstroms and angles in degrees.

TABLE 1: Total Energies (E, hartree), Relative Energies (ΔE, kcal mol^{-1}), Zero-Point Energies (ZPE, kcal mol^{-1}, Unscaled), Thermal Corrections to Enthalpy (H_{th}, kcal mol^{-1}), Activation Energies (E_a, kcal mol^{-1}), and Reaction Enthalpies (ΔH, kcal mol^{-1}) for the Reaction $^{\bullet}SiH_3 + H_2C{=}CH_2$ Computed at the PMP2/6-31G* Level

	E	ΔE	ZPE	H_{th}	E_a or ΔH
reactants	−368.960 05	0.00	46.56	51.51	
TS_1	−368.955 18	3.05	48.48	52.49	5.21
TS_2	−368.909 24	31.88	44.04	48.57	30.12
P_1	−368.993 23	−20.82	48.83	52.88	−19.45
P_2	−368.921 34	24.29	44.69	49.67	22.45

TABLE 2: Total Energies (E, hartree), Relative Energies (ΔE, kcal mol^{-1}), Activation Energies (E_a, kcal mol^{-1}), and Reaction Enthalpies (ΔH, kcal mol^{-1}) for the Reaction $^{\bullet}SiH_3 + H_2C{=}CH_2$ Computed at the QCISD(T) Level with the 6-311G Basis Set**

	E	ΔE	E_a or ΔH
reactants	−369.056 90	0.00	
TS_1	−369.048 48	4.31	6.46
TS_2	−369.015 17	29.13	27.37
P_1	−369.087 58	−20.61	−19.25
P_2	−369.024 79	21.99	20.15

TABLE 3: Total Energies (E, hartree), Relative Energies (ΔE, kcal mol^{-1}), Zero-Point Energies (ZPE, kcal mol^{-1}, Unscaled), Thermal Corrections to Enthalpy (H_{th}, kcal mol^{-1}), Activation Energies (E_a, kcal mol^{-1}), and Reaction Enthalpies (ΔH, kcal mol^{-1}) for the Reaction $^{\bullet}SiH_3 + H_2C{=}CHCH_3$ Computed at the PMP2/6-31G* Level

	E	ΔE	ZPE	H_{th}	E_a or ΔH
reactants	−408.130 56	0.00	65.09	70.71	
TS_1	−408.126 68	2.43	66.80	71.65	4.57
TS_2	−408.123 04	4.72	66.82	71.58	6.78
TS_3	−408.078 53	32.65	62.52	67.87	30.99
TS_4	−408.084 13	29.13	62.54	67.95	27.57
TS_5	−408.079 05	32.32	62.62	67.99	30.79
TS_6	−408.095 84	21.79	62.82	68.04	20.31
TS_7	−408.084 53	28.88	64.44	69.61	28.97
P_1	−408.163 05	−20.39	67.38	72.28	−18.81
P_2	−408.157 94	−17.18	67.14	71.95	−15.93
P_3	−408.090 60	25.07	63.58	69.17	23.54
P_4	−408.096 18	21.57	63.49	69.17	20.05
P_5	−408.090 24	25.30	63.71	68.70	23.31
P_6	−408.131 95	−0.87	62.90	68.34	−3.23

TABLE 4: Total Energies (E, hartree), Relative Energies (ΔE, kcal mol^{-1}), Activation Energies (E_a, kcal mol^{-1}), and Reaction Enthalpies (ΔH, kcal mol^{-1}) for the Reaction $^{\bullet}SiH_3 + H_2C{=}CHCH_3$ Computed at the QCISD(T) Level with the 6-311G Basis Set**

	E	ΔE	E_a or ΔH
reactants	−408.355 56	0.00	
TS_1	−408.350 18	3.37	5.50
TS_2	−408.347 39	5.12	7.17
TS_3	−408.308 54	29.50	27.84
TS_4	−408.313 35	26.48	24.91
TS_5	−408.308 88	29.29	27.76
TS_6	−408.323 61	20.04	18.56
TS_7	−408.315 13	25.37	25.45
P_1	−408.388 54	−20.70	−19.12
P_2	−408.384 03	−17.86	−16.62
P_3	−408.319 92	22.36	20.82
P_4	−408.325 01	19.17	17.64
P_5	−408.319 31	22.74	20.38
P_6	−408.356 22	−0.42	−2.42

responsible for a shorter C_2-C_3 bond distance (1.474 Å) in P_4 than in P_3 and P_5 (1.504 and 1.510 Å).

The accurate prediction of the energy barriers of radical reactions is a difficult problem, and it is well-known that high levels of theory including dynamic correlation are needed to reproduce the experimental results.[7] The QCISD(T) single-point computations with the 6-311G** basis that we have carried out on the MP2/6-31G* geometries represent nowadays a fairly good level of theory and should provide a reference to test the reliability of the PMP2/6-31G* approach for this class of reactions. In the following we discuss the energy results obtained at these two levels of theory, and we compare them with the available experimental results. Inspection of Table 1 shows that the PMP2 level provides for the addition of silyl radical to ethylene an activation energy of 5.21 kcal mol^{-1}, in quite good agreement with the experimental value of about 6 kcal mol^{-1} obtained under the assumption of an A factor of 10^{-10} cm^3 molecule^{-1} s^{-1}.[1f] The PMP2 value is also in good agreement with the QCISD(T) value obtained for E_a (6.46 kcal mol^{-1} in Table 2). Inspection of the remaining results reported in Table 1 shows that the activation energy for vinyl hydrogen abstraction is much higher (30.12 kcal mol^{-1} at the PMP2 level and 27.37 kcal mol^{-1} at the QCISD(T) level). Thus for ethylene the hydrogen transfer corresponds to a high-energy reaction channel that cannot compete with the addition to the C−C double bond.

The energy values of the products P_1 and P_2 show that the addition is an exothermic process: ΔH for P_1 is −19.45 kcal mol^{-1} at the PMP2 level and almost identical at the QCISD(T) level (−19.25 kcal mol^{-1}). These values are in reasonable agreement with the experimental values obtained for $Cl_3Si^{\bullet}$ and ethylene (−16 kcal mol^{-1}) and for $Me_3Si^{\bullet}$ and ethylene (−26 kcal mol^{-1}). On the other hand the abstraction of a vinyl hydrogen is endothermic by 22.45 kcal mol^{-1} (20.15 kcal mol^{-1} at the QCISD(T) level). Also these values are in fairly good agreement with the value of 20 kcal mol^{-1} obtained from the available thermochemistry[8] for these reactions. All these results seem to indicate that a PMP2 approach with a basis set of double-ζ quality in the valence shell plus polarization functions can provide a reliable description of this class of reactions.

The values reported in Tables 3 and 4 show that for propylene the addition reaction channel involving TS_1 is favored with respect to the addition pathway associated with TS_2, the activation energies being 4.57 and 6.78 kcal mol^{-1} respectively at the PMP2 level. The corresponding QCISD(T) values are very similar, being 5.50 and 7.17 kcal mol^{-1} respectively. The lower energy of TS_1 is in agreement with the secondary radical nature of this transition structure and parallels, in agreement with the Hammond postulate, the energies of the corresponding radical products P_1 and P_2 (−18.81 and −15.93 kcal mol^{-1} respectively at the PMP2 level and −19.12 and −16.62 kcal

TABLE 5: Values of $\langle S^2 \rangle$ Computed at the MP2 Level with the 6-31G* Basis Set for the Two Reactions $^{\bullet}SiH_3$ + $H_2C{=}CH_2$ and $^{\bullet}SiH_3$ + $H_2C{=}CHCH_3$

	$^{\bullet}SiH_3 + H_2C{=}CH_2$		
reactants	0.7507	P_1	0.7538
TS_1	0.8860	P_2	0.8948
TS_2	0.8912		
	$^{\bullet}SiH_3 + H_2C{=}CHCH_3$		
reactants	0.7507	TS_7	0.7764
TS_1	0.8760	P_1	0.7539
TS_2	0.8843	P_2	0.7539
TS_3	0.8820	P_3	0.8859
TS_4	0.8690	P_4	0.8722
TS_5	0.8810	P_5	0.8880
TS_6	0.8771	P_6	0.8941

TABLE 6: Vibrational Frequencies (cm^{-1}, Unscaled) Computed at the MP2/6-31G* Level for the Reaction $^{\bullet}SiH_3$ + $H_2C{=}CH_2$

$^{\bullet}SiH_3$	806(A_1)	970(E)	2300(A_1)	2337(E)	
SiH_4	956(E)	957(A_1)	1005(E)	2322(A_1)	2335(T_2)
$H_2C{=}CH_2$	849(B_{2u})	938(B_{2g})	989(B_{3u})	1084(A_u)	1264(B_{3g})
	1414(Ag)	1520(B_{1u})	1719(Ag)	3212(B_{1u})	3229(Ag)
	3298(B_{3g})	3321(B_{2u})			
TS_1	461i	122	161	308	403
	481	851	852	895	975
	982	991	1099	1280	1354
	1524	1650	2238	2300	2318
	3226	3237	3313	3338	
TS_2	1363i	47	101	160	336
	377	524	854	909	971
	977	1023	1054	1099	1117
	1206	1476	1888	2301	2319
	2321	3184	3265	3297	
P_1	170	212	224	466	535
	606	736	793	970	990
	990	1011	1113	1224	1297
	1507	1538	2293	2310	2317
	3102	3163	3239	3349	
P_2	770	993	1064	1121	1465
	1857	3174	3273	3337	

mol^{-1} respectively at the QCISD(T) level). This finding also suggests that in gas phase alkyl substitution slightly enhances the reactivity of olefins toward addition of $^{\bullet}SiH_3$.

The activation energies obtained for the reaction channels leading to vinyl or methyl hydrogen abstraction show that, also for propylene, these processes are highly disfavored. Even if the abstraction of a methyl hydrogen is slightly exothermic (−3.23 and −2.42 kcal mol^{-1} at the PMP2 and QCISD(T) levels respectively, in reasonable agreement with the experimental value of −4.0 ± 2.2 kcal mol^{-1}), the corresponding activation energy remains quite large (20.31 and 18.56 kcal mol^{-1} are the computed PMP2 and QCISD(T) values). This finding definitively rules out the initial hypothesis of Loh et al.[1] that the reaction of silyl radical with propylene may proceed primarily via hydrogen transfer rather than addition and confirms the subsequent and more extensive experiments carried out by these authors.

Finally the S^2 expectation values reported in Table 5 show that a nonnegligible spin contamination affects mainly the transition states. This finding points out the importance of using spin-projected energies to obtain reliable energetics.

B. Diabatic Model. It is interesting to point out that the indication of the gas-phase-enhanced reactivity of the C−C double bond in propylene with respect to ethylene cannot be easily understood in terms of the Hammond postulate since the addition of $^{\bullet}SiH_3$ is slightly less exothermic in the former case (−18.81 kcal mol^{-1}) than in the latter (−19.25 kcal mol^{-1}). However this finding can be rationalized using a simple diabatic model based upon spin recoupling in VB theory.[9] In this model the total energy profile is decomposed into two component curves: one, associated with the reactant spin-coupling (reactant bonding situation), is indicated as *reactant diabatic*, and the other, associated with the product spin-coupling (product bonding situation), is denoted as *product diabatic*. Along the reaction coordinate the behavior of the reactant diabatic is repulsive and that of the product diabatic is attractive. The crossing of the two curves detects the transition state and the energy barrier.

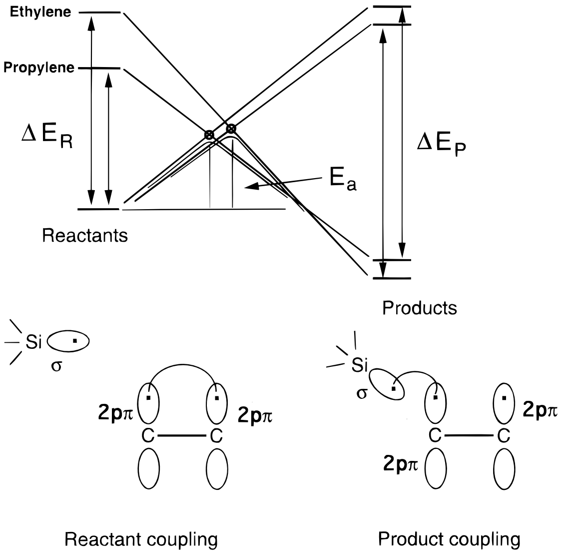

Figure 5. Correlation diagram for the two addition reactions $^{\bullet}SiH_3$ + $H_2C{=}CH_2$ and $^{\bullet}SiH_3$ + $H_2C{=}CHCH_3$.

In Figure 5 we have represented the qualitative behavior of the two diabatics for the addition of the silyl radical $^{\bullet}SiH_3$ to ethylene and propylene. The reactant diabatic describes a situation where the two 2pπ orbitals centered on C_1 and C_2 are singlet spin-coupled to form the olefin bond (reactant coupling), while the product diabatic corresponds to a singlet spin-coupling between the σ orbital on the silyl radical and the 2pπ orbital centered on one olefinic carbon (product coupling).

The diagrams reported in Figure 5 are based on the following assumptions:

(i) The product diabatics at the product geometry are positioned with respect to the reactant diabatics at the reactant geometry on the basis of the reaction energies (ΔH) reported in Tables 1−4.

(ii) A common reference energy level for reactants has been assumed in the two cases.

(iii) The energy difference between reactant diabatic and product diabatic at the product geometry (ΔE_P on the right side of the diagram) has been assumed to be identical for ethylene and propylene. This quantity depends only on the coupling/decoupling between the two electrons involved in the new Si−C bond and thus can be evaluated to a good approximation from the corresponding bond energy: the identical value (1.902 Å) of the Si−C bond length in the two product radicals $H_3Si{-}CH_2{-}CH_2^{\bullet}$ and $H_3Si{-}CH_2{-}CH(CH_3)^{\bullet}$ suggests that this bond energy is almost identical in the two cases.

(iv) The energy difference between the two diabatics at the reactant geometry (ΔE_R on the left side of the diagram) depends on the coupling/decoupling between the two 2pπ carbon orbitals in ethylene and propylene and can be evaluated to a good approximation from the energies of the vertical $\pi \rightarrow \pi^*$ triplet excitation in the two molecules. This quantity is 99.1 kcal mol^{-1} in ethylene, while a batochromic effect due to the methyl group is observed in propylene where this value is shifted to 97.5 kcal mol^{-1}.[10]

TABLE 7: Vibrational Frequencies (cm^{-1}, Unscaled) Computed at the MP2/6-31G* Level for the Reaction $^{\bullet}SiH_3$ + $H_2C{=}CHCH_3$

$H_2C{=}CHCH_3$	199	431	592	928	957
	974	1041	1105	1227	1357
	1464	1502	1544	1559	1742
	3097	3173	3192	3206	3215
	3302				
TS_1	474i	97	126	155	216
	382	426	442	721	854
	884	965	973	980	988
	1074	1104	1239	1341	1460
	1493	1538	1554	1664	2226
	2290	2308	3093	3166	3200
	3217	3233	3310		
TS_2	519i	115	168	182	241
	398	414	472	594	854
	910	944	974	978	988
	1046	1086	1229	1329	1463
	1498	1549	1558	1645	2220
	2293	2313	3105	3187	3210
	3225	3228	3324		
TS_3	1354i	13	92	99	212
	289	306	428	545	690
	906	954	972	975	986
	1018	1026	1119	1146	1204
	1350	1468	1547	1555	1955
	2297	2315	2316	3109	3137
	3184	3224	3291		
TS_4	1387i	39	76	107	199
	249	337	343	540	654
	904	955	973	976	998
	1038	1045	1123	1140	1201
	1453	1491	1529	1545	2030
	2296	2315	2315	3083	3171
	3171	3189	3261		
TS_5	1260i	41	69	81	217
	274	300	373	592	738
	907	964	970	972	990
	1012	1045	1139	1154	1192
	1362	1463	1544	1553	1947
	2299	2316	2318	3103	3183
	3183	3212	3282		
TS_6	1918i	26	68	109	224
	306	376	454	637	688
	882	972	976	980	1021
	1033	1068	1138	1217	1226
	1240	1386	1492	1532	1773
	2290	2312	2315	3175	3211
	3226	3270	3316		
TS_7	1594i	6	104	106	249
	302	394	522	536	725
	901	976	976	990	1002
	1061	1116	1146	1161	1181
	1210	1391	1511	1526	2293
	2313	2313	2801	3179	3179
	3267	3314	3320		
P_1	73	130	146	228	384
	455	538	603	738	863
	933	969	990	990	992
	1040	1069	1196	1226	1260
	1436	1480	1508	1541	1557
	2293	2308	2313	3055	3089
	3134	3150	3189	3247	
P_2	162	216	232	240	289
	378	484	596	655	715
	925	960	964	985	990
	1050	1151	1201	1258	1372
	1466	1526	1559	1568	2284
	2304	2312	3090	3097	3184
	3189	3225	3336		
P_3	217	426	687	864	969
	978	1140	1170	1334	1468
	1548	1555	1919	3109	3139
	3186	3220	3336		
P_4	206	336	558	937	987
	1018	1113	1163	1452	1483
	1528	1543	2001	3078	3157
	3171	3199	3272		
P_5	214	403	735	909	974
	991	1142	1154	1336	1462
	1546	1555	1904	3107	3187
	3200	3215	3322		
P_6	441	562	591	804	822
	969	1058	1083	1171	1333
	1456	1546	1585	3225	3230
	3238	3337	3339		

This model shows that the entity of the barrier is due to the combined effect of two factors: the reaction enthalpy (as indicated by the Hammond postulate) and the $\pi \rightarrow \pi^*$ triplet excitation energy. Since in the present case the change of the reaction enthalpy on passing from ethylene to propylene is negligible, while the excitation energy varies more significantly and in the opposite direction, the final effect of the alkylation of the double bond is that of slightly decreasing the energy barrier for the addition of silyl radical in agreement with the computational results.

The better performance of the diabatic model with respect to a model based on the Hammond postulate (which would predict almost the same activation energy in the two cases) depends on the fact that, in determining the transition state and the entity of the barrier, the diabatic model can take into account not only the reaction enthalpies but also other factors as the energies of the forming and breaking bonds (in the present case the energy of the π bond). Thus only when the trend of these additional factors parallels that of the reaction enthalpies or when the reaction enthalpies represent the dominating factor can the two models provide the same answer.

The slightly enhanced reactivity of propylene is apparently in contrast with the decreasing reactivity experimentally observed in solution for the reaction between triethylsilyl radicals and 1-alkyl-substituted olefins.[3a] However this experimentally observed trend can be explained on the basis of the steric repulsion between the approaching silyl radical and the alkyl-substituted olefin. Since this repulsion should be larger in the case of the bulky $^{\bullet}SiEt_3$ radical than for $^{\bullet}SiH_3$, the slope of the reactant diabatic for the reaction between alkyl-substituted olefins and $^{\bullet}SiEt_3$ increases and so does the activation barrier.

Conclusions

In this paper we have investigated using both a PMP2 approach with the 6-31G* basis set and a QCISD(T) approach with the more accurate 6-311G** basis set, the potential energy surfaces associated with the reactions of the silyl radical $^{\bullet}SiH_3$ with ethylene and propylene. We have found that in both cases the reaction channels leading to the olefin double-bond addition are highly favored with respect to the reaction pathways associated with hydrogen abstraction. Also the abstraction of a methyl hydrogen in the case of propylene is characterized by a significant activation energy (about 19 kcal mol^{-1}) even if the process, which leads to the formation of an allyl radical, is slightly exothermic. These results rule out the hypothesis that hydrogen abstraction and not double-bond addition is the primary process in the case of propylene in agreement with the more recent and more accurate experimental results obtained by Loh et al.[1f] However in the comparison between ethylene and propylene we have found that the addition reaction is slightly favored in the latter case as compared to the former. Thus also this factor should probably be taken into account to explain the higher rate constant found for propylene by Loh and co-workers.[1f]

Another point of interest is represented by the good agreement between the computed reaction energetics and the experimental values available for these reactions (activation energies, reaction exothermicities, and endothermicities). The comparison between the results obtained at the PMP2 and the QCISD(T) levels indicates that a PMP2 computational approach with a basis set of double-ζ quality plus polarization functions (6-31G*) can provide a reliable description for this class of reactions.

Finally we have demonstrated that the computational results (lower activation energy for the addition reaction in the case of propylene) can be rationalized using a simple diabatic model. We have demonstrated that in this case this model performs better than a model based on the Hammond postulate which takes into account only the reaction enthalpies which are very similar for the two reactions. In the present case the diabatic model indicates the $\pi \rightarrow \pi^*$ triplet excitation energy as the key factor which determines the trend of the gas-phase activation barrier on passing from ethylene to propylene.

References and Notes

(1) (a) Sommer, L. H.; Pietrusza, E. W.; Whitmore, F. C. *J. Am. Chem. Soc.* **1947**, *69*, 188. (b) Burkhard, C. A.; Krieble, R. H. *J. Am. Chem. Soc.* **1947**, *69*, 2687. (c) Barry, A. J.; De Pree, L.; Gilkey, J. W.; Hook, D. E. *J. Am. Chem. Soc.* **1947**, *69*, 2916. (d) Sakuray, H. In *Free radicals*; Kochi, J. K., Ed.; Wiley: New York, 1973; Vol II, p 741. (e) Alberti, A.; Pedulli, G. *Rev. Chem. Instrum.* **1978**, *8*, 207. (f) Loh, S. K.; Beach, D. B.; Jasinski, J. M. *Chem. Phys. Lett.* **1990**, *169*, 55. (g) Chatgilialoglu, C. *Chem. Rev.* **1995**, *95*, 1229. (h) Jasinski, J. M.; Becerra, R.; Walsh, R. *Chem. Rev.* **1995**, *95*, 1203.

(2) (a) Bennet, S. W.; Eaborn, C.; Jackson, R. A.; Pearce, R. *J. Organomet. Chem.* **1968**, *15*, P17. (b) Jackson, R. A. *J. Chem. Soc., Chem. Commun.* **1974**, 573.

(3) (a) Chatgilialoglu, C.; Ingold, K. U.; Scaiano, J. C. *J. Org. Chem.* **1983**, *105*, 3292. (b) Chatgilialoglu, C.; Ingold, K. U.; Lusztyk, J.; Nazran, A. S.; Scaiano, J. C. *Organometallics* **1983**, *2*, 1332. (c) Ballestri, M.; Chatgilialoglu, C.; Clark, K. B.; Griller, D.; Giese, B.; Kopping, B. *J. Org. Chem.* **1991**, *56*, 678.

(4) (a) Aloni, R.; Rajbenbach, L. A.; Horowitz, A. *J. Organomet. Chem.* **1979**, *171*, 155. (b) Horowitz, A. *J. Am. Chem. Soc.* **1985**, *107*, 318.

(5) Frisch, M. J.; Trucks, G. W.; Schlegel, H. B.; Gill, P. M. W.; Johnson, B. G.; Wong, M. W.; Foresman, J. B.; Robb, M. A.; Head-Gordon, M.; Replogle, E. S.; Gomperts, R.; Andres, J. L.; Raghavachari, K.; Binkley, J. S.; Gonzalez, C.; Martin, R. L.; Fox, D. J.; Defrees, D. J.; Baker, J.; Stewart, J. J. P.; Pople, J. A. *Gaussian 92/DFT*, Revision G.1; Gaussian, Inc.: Pittsburgh, PA, 1993.

(6) (a) Hariharan, P. C.; Pople, J. A. *Theor. Chim. Acta* **1973**, *28*, 213. (b) Krishnan, R.; Binkley, R. S.; Seeger, R.; Pople, J. A. *J. Chem. Phys.* **1980**, *72*, 650. McLean, A. D.; Chandler, G. S. *J. Chem. Phys.* **1980**, *72*, 5639.

(7) Sosa, C.; Schlegel, H. B. *Int. J. Quantum Chem.* **1986**, *29*, 1001; **1987**, *30*, 155.

(8) McMillen, D. F.; Golden, D. M. *Annu. Rev. Phys. Chem.* **1982**, *33*, 493. Walsh, R. *Acc. Chem. Res.* **1981**, *14*, 246.

(9) Pross, A.; Schaik, S. S. *Acc. Chem. Res.* **1983**, *16*, 363. Bernardi, F.; Olivucci, M.; McDouall, J. J. W.; Robb, M. A. *J. Chem. Phys.* **1988**, *89*, 6365.

(10) Johnston, K. E.; Johnston, D. B.; Sanford, L. *J. Chem. Phys.* **1979**, *70*, 3844.